Pattern formation on carbon nanotube surfaces

Article (Published Version)

Pattern Formation on Carbon Nanotube Surfaces

Chris P. Ewels,[1,2,*] Gregory Van Lier,[3] Jean-Christophe Charlier,[3] Malcolm I. Heggie,[4] and Patrick R. Briddon[5]

[1]*LPS, CNRS UMR8502, Université Paris Sud, Batîment 510, 91405 Orsay, France*
[2]*Institut des Matériaux Jean Rouxel, CNRS-Université de Nantes, UMR6502, 2 Rue de la Houssinière, BP 32229, 44322 Nantes, France*
[3]*Université Catholique de Louvain, PCPM & CERMIN, Place Croix du Sud 1, B-1348 Louvain-la-Neuve, Belgium*
[4]*Department of Chemistry, School of Life Sciences, Sussex University, Brighton BN1 9QJ, United Kingdom*
[5]*School of Natural Sciences, University of Newcastle Upon Tyne, Newcastle NE1 7RU, United Kingdom*

(Received 14 December 2005; published 31 May 2006)

Calculations of fluorine binding and migration on carbon nanotube surfaces show that fluorine forms varying surface superlattices at increasing temperatures. The ordering transition is controlled by the surface migration barrier for fluorine atoms to pass through next neighbor sites on the nanotube, explaining the transition from semi-ionic low coverage to covalent high coverage fluorination observed experimentally for gas phase fluorination between 200 and 250 °C. The effect of solvents on fluorine binding and surface diffusion is explored.

DOI: 10.1103/PhysRevLett.96.216103 PACS numbers: 81.16.Rf, 61.46.Fg, 68.35.Rh, 68.43.Bc

Chemical functionalization of carbon nanotubes (CNTs) provides an important route to the development of novel materials [1]. Of the available methods, fluorination is emerging as an important process for functionalizing and chemically activating CNTs [2]. Fluorinated nanotubes can be used as precursors for further functionalization [3,4] and are soluble in a variety of common solvents [3,5], aiding tube bundle separation and purification. Potential applications for fluorinated nanotubes include use as electrodes in lithium-ion batteries [6], supercapacitors [7], and lubricants [8–10].

There are various ways to fluorinate CNTs, including gas phase routes using atomic fluorine [5], F_2 gas [11], BF_3 vapor [12], and CF_4 plasma functionalization [13]. Fluorine coverage of single walled CNTs increases with increasing temperature, reaching a maximum coverage of C_2F between 250 and 300 °C [14,15]. At higher temperatures the tubes break down into graphitic material where coverage can approach CF [16]. X-ray photoelectron spectroscopy (XPS) studies show a change in C-F bonding type between 200 and 250 °C. Up to 200 °C the XPS spectra are centered at 688 eV (semi-ionic fluorination), whereas at 250 °C the peak shifts to 691 eV (covalentlike fluorination) [14,15]. The change is reflected in the F/C ratio which jumps from 0.20–0.25 at 200 °C to 0.5 at 250 °C, while sample resistivity increases by a factor of 3 [15].

To date, most theoretical studies of nanotube fluorination have concentrated on the maximum C_2F fluorine coverage [17–19]. Different addition patterns were studied in order to confirm the experimentally observed circumferential banding at high fluorine coverage [2,17]; however, most theoretical studies predict axial addition as more stable [see Fig. 1(a)]. This discrepancy was recently explained via contiguous fluorine addition in axial rows [20]. Although the fluorine forms axially oriented rows, these parallel rows match lengths, providing a sharp circumferential edge between fluorinated and nonfluorinated regions that minimizes strain in the host nanotube.

Jaffe used small hydrocarbons to simulate nanotube sidewalls [19]. His binding energy for isolated F (compared to gas phase F_2) was ≈ 0.41 eV, with a F surface migration barrier of 0.54 eV. For 2 F atoms he found a (1,2) arrangement most stable, with (1,3) very unstable [for notation, see Fig. 1(c)]. The binding energy per F atom increased with further F addition, shifting to 0.97, 0.94, and 1.31 eV/F for 2, 3, and 4 F atoms, respectively.

No calculations have yet addressed the change in fluorination behavior between 200 and 250 °C, or the apparent 20%–25% surface concentration limit at lower temperatures. In addition, there remain other questions such as the atomic nature of semi-ionic and covalent fluorine bonding. In this Letter we attempt to address these questions through density functional calculations of large nanotube sections. We model isolated and pairwise fluorine addition, associated migration barriers, and calculate XPS signals. The temperature transition is shown to arise from the barrier for fluorine migration on the nanotube surface, which blocks dense packing and nanotube fluorine banding at lower temperatures. Fluorine bonding shows two different bonding types, depending on whether the fluorine is dense packed. XPS simulations confirm that these correspond to experimentally observed covalent and semi-ionic fluorination, respectively. Finally, the influence of solvents on fluorine behavior is explored, using water as an example.

We perform pseudopotential [21] local density functional AIMPRO calculations [22] of fully optimized (8,8) carbon nanotubes, using periodically repeated 192 carbon atom sections (5 bands of armchair hexagons) with different numbers of surface fluorine atoms. AIMPRO has previously been used to study defects in graphite [23] and fluorinated fullerenes [24]. Diffusion barriers are calculated by constraining the difference of the squares of the

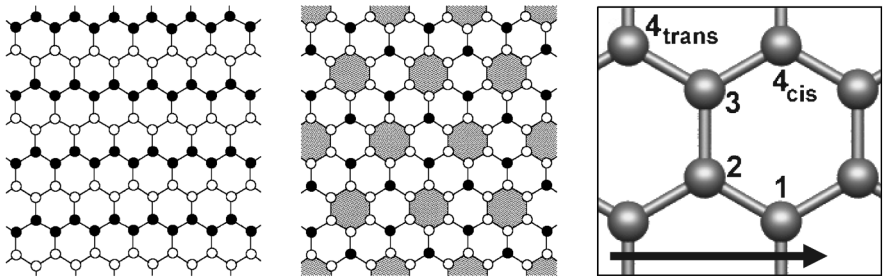

FIG. 1. Schematic diagrams of (a) C_2F and (b) C_4F. Solid (open) circles denote (un)fluorinated carbon atoms. C_4F is the maximum coverage with no fluorinated carbon atoms at second neighbor spacing. (c) The notation (x, y) in this Letter indicates fluorine atoms bonded to carbon atoms x and y in the diagram above. The arrow marks the nanotube axis.

distances between an F atom and each of two neighboring C atoms to be a constant x, and otherwise allowing full geometrical optimization of 10 atoms around the defect. By varying x we can track the energy pathway as the F breaks one C-F bond and forms another. Binding energies are quoted, except where stated otherwise, with respect to an isolated perfect nanotube and fluorine in an F_2 molecule. For comparison, graphene calculations are performed on 128 atom periodic sheets separated by over 8 Å.

Our calculations for a single surface F atom on the (8,8) nanotube give a C-F bond length of 1.455 Å and binding energy of 1.43 eV (see Table I). Thus, as expected, the binding energies on a nanotube are higher than for graphite (0.99 eV) (since curvature makes the carbon atoms less aromatic and more reactive), and lower than for C_{60} ($\sim$4 eV) [25]. The binding energy for C_2F coverage in axial bands of the same tube is 1.83 eV/F, with bond lengths of 1.385 Å, approaching CF graphene fluoride (1.363 Å).

We next explore a pair of fluorine atoms. Fluorine bonded to carbon at sites (1,2), (1,3), and $(1, 4_{cis})$ are the lowest energy configurations for fluorine atoms at first, second, and third neighbor spacing, respectively [see Fig. 1(c)]. The most stable is (1,2), followed by the $(1, 4_{cis})$ and (1,3), respectively, consistent with previous studies [20], with bond lengths varying between the single F and C_2F extremes (see Table I). The (1,3) configuration is significantly less stable than the others, since the radicals created by each F atom lie on the same sublattice of carbon sites and so cannot restore the π network, comparable with the metaposition for addition to benzene.

XPS values are obtained by comparison of the total self-consistent system energy between a fluorinated structure and the same structure with one F replaced by Ne in a +1 charge state, after correcting for background cell charge. These values are shifted to align the C_2F value with the experimentally observed XPS F(1s) peak at 691 eV [15]. These experimental spectra ranging from 150 to 300 °C show a shift between 200 and 250 °C, with higher temperature peaks centered at 690.7 with a shoulder at 688 eV, and lower temperature peaks between 687 and 687.6 eV, with a 685 eV shoulder in the 150 °C peak.

Our calculated XPS F(1s) energies fall into two broad categories: 691 eV associated with C_2F, and lower energy values between 686 and 687 eV for isolated single and paired F atoms, suggesting that the XPS covalently bonded fluorine signal is associated with C_2F, whereas the semi-ionic signal is due to lower density coverage. This is consistent with the long CF bonds for isolated F, short bonds for C_2F, and intermediate lengths for fluorine pairs. Our calculated XPS peak for isolated F lies at 685.7 eV, whereas the F pair XPS peak energies lie $\sim$1 eV higher at 686.6–686.9 eV. This suggests that the shoulder at 685 eV in the experimental 150 °C spectrum [15] may be due to isolated fluorine on the tube surface.

In order to understand the transition between 200 and 250 °C when fluorinating CNTs we next examined F sur-

TABLE I. Calculated fluorine binding energies (eV), bond lengths (Å), and F(1s) XPS peak (eV) in different configurations on graphene and an (8,8) nanotube. F_2 (x, y) indicates fluorine atoms bonded to atoms x and y in Fig. 2. Binding energies relative to F_2 and nanotube or graphene as appropriate. F(1s) XPS values are linearly shifted to align C_2F with experiment [15]. For reference, fully fluorinated graphene (CF) has binding energy 2.10 eV/F, C-F bond length 1.363 Å.

	(8,8) nanotube			Graphene	
Fluorine environment	Binding energy/F (eV)	C-F bond length (Å)	F(1s) XPS peak (eV)	Binding energy/F (eV)	C-F bond length (Å)
F	1.43	1.455	685.7	1.04	1.495
F_2 $(1, 4_{cis})$	2.38	1.435	686.6	1.40	1.458
F_2 $(1, 4_{trans})$				1.10	1.486
F_2 (1,3)	1.87	1.466	685.5	1.00	1.499
F_2 (1,2)	2.43	1.408	686.9	1.37	1.431
C_4F	1.75	1.410			
C_2F	1.83	1.385	691.0		

face migration. Migration barriers will be curvature dependent, since curvature will modify the ground state binding energies but have less of an effect on the saddle point energy. For this reason we examined F migration on both an (8,8) nanotube and a graphene sheet in order to bracket the range of experimental tube radii.

Isolated neutral F atoms diffuse rapidly on graphene (barrier 0.50 eV) along a path above C-C bonds [close to previous (10,0) nanotube calculations [19]]. On the nanotube this migration barrier depends on whether motion is axial (0.79 eV) or circumferential (0.94 eV); the ground state sites of the fluorine are more distant in the circumferential case.

Now we turn to 2 F atoms in proximity. The migration barriers to move one of the F atoms of a pair from first to second neighbor on a graphene sheet is 1.35 eV, and from third to second is 1.18 eV (see Fig. 2). Thus close packing of fluorine on a graphene surface is possible only once a 1.35 eV barrier has been surmounted. The equivalent values for the (8,8) nanotube are 1.74 and 1.31 eV, respectively. We have considered only barriers between the lowest energy first, second, and third neighbor configurations on the nanotube, although as for single F migration there will be some variation depending on nanotube chirality and whether migration is axial or circumferential.

These barriers suggest isolated F will migrate rapidly over the nanotube surface, settling to sit as third neighbor $(1, 4_{cis})$ pairs. Thereafter the fluorine atoms will not be able to approach any closer until they are able to pass through the (1,3) pair configuration. Equally fluorine pairs in the (1,2) arrangement have to pass through the (1,3) pair structure in order to move over the nanotube surface. Therefore in order to allow fluorine close packing on the nanotube surface the atoms will need to clear the migration barrier associated with the (1,3) arrangement, i.e., 1.35 eV in graphene or 1.74 eV in an (8,8) nanotube.

Considering simple first order Arrhenius-type diffusion where fluorine hop rate equals $\nu_o \exp(-E/kT)$, if we take

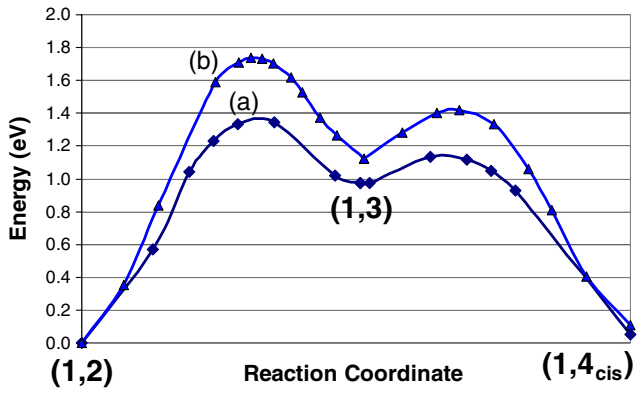

FIG. 2 (color online). Activation barriers (eV) for two fluorine atoms to migrate together over (a) graphene and (b) (8,8) carbon nanotube. (x, y) indicates fluorine atoms bonded to carbon atoms x and y in Fig. 1(c). The (1,3) fluorine spacing and associated barriers block close packing of fluorine at lower temperatures.

ν_o, the attempt frequency, to be the Debye frequency 10^{13} Hz, the migration barrier E to be 1.35 eV from graphene (i.e., larger radius tubes), and a hop rate of 1 hop/s consistent with the slow experimentally observed fluorination rates, this gives an associated temperature T of 230 °C, in good agreement with the experimentally observed transition in behavior between 200 and 250 °C. Thus we suggest that the experimentally observed shift in properties in this temperature range corresponds to the temperature at which fluorine pairs can migrate into and through the metastable second neighbor configuration. The higher barrier for the (8,8) tube suggests that full C_2F fluorine coverage temperature is a function of nanotube radius, and that the transition temperature is gradual based on the distribution of tube diameters.

The second neighbor barrier to migration below 200–250 °C will preclude close aggregation of isolated fluorine atoms. Full surface coverage when fluorine proximity is restricted to $(1, 4_{cis})$ third neighbor produces a F/C ratio of at most 0.25 (C_4F), an equivalent arrangement to that proposed for BC_3 [26] [see Fig. 1(b)]. In practice, different addition patterns are likely to coexist, resulting in a global F/C ratio consistent with the experimentally observed maximum coverage below 250 °C of 20% to 25% [7,14,17]. However, as fluorine surface coverage increases, the average binding energy per F atom drops; our calculations for C_4F give a binding energy per F of 1.75 eV for the (8,8) nanotube. Thus there is a thermodynamic driving force at these higher coverages towards C_2F [see Fig. 1(a)], where binding energy per F is 1.83 eV.

Above 200–250 °C fluorine can migrate freely and aggregate into domains minimizing tube strain energy and maximizing sp^3 hybridization of the fluorinated carbon [20]. This allows surface coverage to increase towards the experimentally observed maximum of 50%, C_2F [Fig. 1(a)]. Thus the calculations predict that the presence of an unstable intermediate structure blocks surface rearrangement of the fluorine, leading instead to a metastable third neighbor surface coverage [i.e., $(1, 4_{cis})$ addition]. It would be interesting to see if such metastable structures occur in other materials where surface species diffusion is important.

HF is a common catalyst in nanotube fluorination [5]. When we place a HF molecule close to F_2 on the graphene surface in our calculations, the F_2 spontaneously breaks, 1 F atom forming a 1.440 Å C-F bond with the graphene, the remaining atoms forming the linear molecule FHF, which is repelled from the F. This arrangement is 2.19 eV lower in energy than HF and F_2 as separated molecules on the same graphene sheet. FHF can then later lose an F atom, restoring HF for further catalysis. This mechanism suggests that HF catalyzed F_2 addition will not lead to next neighbor F bonding but at closest $(1, 4_{cis})$ F pairs, or more likely isolated F addition to the tube surface.

There remain some unaddressed questions concerning low temperature carbon nanotube fluorination. STM studies show dense C_2F fluorine banding after fluorination at

250 °C. Such banding is also observed at 150 °C, with spaced bands corresponding to ~25% F coverage [17]. In this case the tubes were dispersed in solvent (isopropanol or DMF) and sonicated before viewing. The observed ~25% F coverage is consistent with gas phase coverage at third neighbor which then rearranges into bands on exposure to the solvents. Equally, F on C_{60} can rearrange itself for certain isomers at room temperature when in solution [27]. Both suggest F surface migration may have a lower barrier in the presence of solvents.

In order to investigate this, we performed exploratory calculations of binding and migration of 1 and 2 F atoms on the graphene surface in the presence of a single water molecule. H_2O has a 0.2 eV binding energy to graphene-F (0.0 eV on pristine graphene), consistent with the observed water solubility of fluorinated nanotubes. F migration between a (1,2) and a (1,3) F_2 pair, allowing unconstrained geometrical optimization of a neighboring water molecule throughout the diffusion path, showed a decrease in the migration barrier of 0.4 eV. Solvents that transfer charge to the nanotube surface will facilitate F migration; when we repeated our calculations for a single F atom on graphene with an additional electron in the system, the migration barrier decreased by 0.26 eV.

This raises the interesting possibility of low temperature solvent based routes for nanotube fluorination, either for direct fluorination or as a posttreatment to allow surface rearrangement. In this case overall fluorine coverage could be controlled during fluorination, and the banding controlled through the solvation conditions.

In summary, these results suggest varying fluorine behavior depending on the temperature, charge state, and curvature of the host carbon substrate. Surface fluorine atoms rapidly migrate at low temperatures before pairing up at third neighbor spacings, showing semi-ionic bonding. Increasing fluorine coverage at third neighbor leads to a maximum F/C surface coverage of 0.25 [Fig. 1(a)]. As the temperature is increased to between 200 and 250 °C, fluorine can overcome the activation barrier associated with adopting the energetically unfavorable second neighbor configuration, enabling a new phase with close packing at first neighbor [Fig. 1(b)]. This close packing allows F to form axially oriented chains along the nanotube, with short highly covalent CF bonds as identified in XPS. These chains arrange into bands of axial CF with abrupt circumferential edges, eventually covering the tube exterior with F/C ratio of 0.5 under further F addition.

Curvature increases F binding and correspondingly migration barriers. Polar solvents that bind to F such as water molecules can also act to stabilize the saddle point structures and so lower migration barriers. Controlled solvation of low temperature fluorinated tubes, possibly in the presence of alternative surface addends, could allow tailoring of surface fluorine band properties such as their band widths. This would result in tubes with regular polar or nonpolar regions along their length, with many potential applications in composites and nanoelectronics.

We thank A. De Vita, A. El-Barbary, and the group of C. Colliex for useful discussions. C. P. E. is partly supported by a Marie Curie Fellowship. J.-C. C. thanks the Belgian FNRS for financial support. Parts of this work are directly connected to the ENABLE project financed by the Région Wallone de Belgique and to the NANOQUANTA and FAME European networks of excellence.

*Corresponding author.
Electronic address: chris@ewels.info

[1] J. L. Bahr and M. J. Tour, J. Mater. Chem. **12**, 1952 (2002).
[2] V. N. Khabashesku, W. E. Billups, and J. L. Margrave, Acc. Chem. Res. **35**, 1087 (2002).
[3] E. T. Mickelson *et al.*, J. Phys. Chem. B **103**, 4318 (1999).
[4] K. R. Saini *et al.*, J. Am. Chem. Soc. **125**, 3617 (2003).
[5] E. T. Mickelson *et al.*, Chem. Phys. Lett. **296**, 188 (1998).
[6] A. Hamwi *et al.*, Mol. Cryst. Liq. Cryst. Sci. Technol., Sect. A **310**, 185 (1998).
[7] J. Y. Lee *et al.*, J. Phys. Chem. B **107**, 8812 (2003).
[8] T. Hayashi *et al.*, Nano Lett. **2**, 491 (2002).
[9] V. Gupta, Nano Lett. **4**, 999 (2004).
[10] T. Hayashi, Nano Lett. **4**, 1001 (2004).
[11] P. R. Marcoux *et al.*, Phys. Chem. Chem. Phys. **4**, 2278 (2002).
[12] N. F. Yudanov *et al.*, Chem. Mater. **14**, 1472 (2002).
[13] A. Felten, C. Bittencourt, G. Van Lier, J.-C. Charlier, and J. J. Pireaux, J. Appl. Phys. **98**, 074308 (2005).
[14] K. H. An *et al.*, Appl. Phys. Lett. **80**, 4235 (2002).
[15] Y. S. Lee, T. H. Cho, B. K. Lee, J. S. Rho, K. H. An, and Y. H. Lee, J. Fluorine Chem. **120**, 99 (2003).
[16] A. Hamwi *et al.*, Carbon **35**, 723 (1997).
[17] K. F. Kelly *et al.*, Chem. Phys. Lett. **313**, 445 (1999).
[18] K. N. Kudin, G. E. Scuseria, and B. I. Yakobson, Phys. Rev. B **64**, 235406 (2001).
[19] R. L. Jaffe, J. Phys. Chem. B **107**, 10 378 (2003).
[20] G. Van Lier, C. P. Ewels, F. Zuliani, A. De Vita, and J.-C. Charlier, J. Phys. Chem. B **109**, 6153 (2005).
[21] C. Hartwigsen, S. Goedecker, and J. Hutter, Phys. Rev. B **58**, 3641 (1998).
[22] P. R. Briddon and R. Jones, Phys. Status Solidi B **217**, 131 (2000).
[23] R. H. Telling, C. P. Ewels, A. A. El-Barbary, and M. I. Heggie, Nat. Mater. **2**, 333 (2003).
[24] P. A. Troshin *et al.*, Science **309**, 278 (2005).
[25] G. Van Lier, M. Cases Amat, C. P. Ewels, R. Taylor, and P. Geerlings, J. Org. Chem. **70**, 1565 (2005).
[26] J. Kouvetakis, R. B. Kaner, M. L. Sattler, and N. Bartlett, J. Chem. Soc. Chem. Commun. **24**, 1758 (1986).
[27] A. G. Avent and R. Taylor, Chem. Commun. (Cambridge) **22**, 2726 (2002).